Application of CRISPR/Cas9-based mutant enrichment technique to improve the clinical sensitivity of plasma *EGFR* testing in patients with non-small cell lung cancer

Boyeon Kim
Gangnam Severance Hospital
Yoonjung Kim
Gangnam Severance Hospital
Saeam Shin
Yonsei University College of Medicine
Seung-Tae Lee
Yonsei University College of Medicine
Jae Yong Cho
Gangnam Severance Hospital
Kyung-A Lee (kal1119@yuhs.ac)
Gangnam Severance Hospital

Research

Keywords: Cell-free nucleic acids, EGFR gene, liquid biopsy, CRISPR-Cas System, non-small cell lung cancer

Posted Date: September 28th, 2021

DOI: https://doi.org/10.21203/rs.3.rs-927246/v1

Version of Record: A version of this preprint was published at Cancer Cell International on February 15th, 2022. See the published version at https://doi.org/10.1186/s12935-022-02504-2.

Abstract

Background

Mutation detection in cell-free DNA (cfDNA) has increased and is becoming important in the field of precision medicine. Highly fragmented, low-quantity circulating tumor DNA is an obstacle for detecting mutations. Therefore, more sensitive mutation detection techniques are required. Here, we report a new mutant enrichment technology, the CRISPR system combined with post-polymerase chain reaction (PCR) cfDNA (CRISPR-CPPC) to detect the T790M mutation using droplet digital PCR (ddPCR) from cfDNA with extremely low mutant allele copies.

Methods

The CRISPR-CPPC process comprises the following three steps: (1) cfDNA PCR, (2) assembly of post-PCR cfDNA and CRISPR/CRISPR associated protein 9 complex, and (3) enrichment of the target DNA template. After CRISPR-CPPC, the target DNA can be detected using a variety of downstream applications. We optimized and validated CRISPR-CPPC using reference cfDNA standards and cfDNA from patients with non-small cell lung cancer (NSCLC) who underwent tyrosine kinase inhibitor (TKI) therapy. We then compared the detection sensitivity of CRISPR-CPPC with the results of real-time PCR (qPCR) and those of ddPCR without CRISPR-CPPC.

Results

CRISPR-CPPC aided detection of T790M with 93.9% sensitivity and 100% specificity in patients with progressive disease. Using CRISPR-CPPC, T790M mutant copies were sensitively detected by ddPCR, achieving an approximately 13-fold increase in the detected allele frequency.

Conclusions

When tested in patients with progressive disease, the performance of CRISPR CPPC was exceptionally higher than that of other currently available methods. CRISPR-CPPC can greatly contribute to diagnosis and the selection of appropriate treatment regimens by facilitating the sensitive detection of mutations in cfDNA.

Background

Liquid biopsy for detecting circulating tumor DNA (ctDNA) has been most commonly implemented for detecting epidermal growth factor receptor (*EGFR*) mutations in non-small cell lung cancer (NSCLC) [1]. However, highly fragmented and low-quantity ctDNA, high background of wild-type (WT) alleles and the rapid clearance of cell-free DNA (cfDNA) are obstacles for detecting especially low allele frequency

mutations in cfDNA [2, 3]. Sensitive detection of T790M resistance mutation may help to select third-generation EGFR-TKI as a second-line treatment in NSCLC patients with progressive disease (PD) after being administered with first-line tyrosine kinase inhibitors (TKIs) [4–6]. Generally, ≥ 10 copies/mL of T790M can be detected by currently available methods, but most patients have a low T790M copy number (< 10 copies/mL), making T790M difficult to detect [7]. Nevertheless, patients with a low T790M copy number (< 10 copies/mL) have a similar response to third-generation EGFR-TKIs as those with a higher T790M copy number (≥ 10 copies/mL) [8].

For patients with NSCLC, real-time PCR (qPCR), such as FDA-approved Roche cobas® EGFR Mutation Test v2 (Roche Molecular Systems, Pleasanton, CA, USA), is widely used in the clinical setting because of its ease of use and relatively low cost. However, the test requires at least 100 copies/mL of specific *EGFR* mutants for the sensitive detection of mutations [9]. If the mutant allele frequency of *EGFR* mutants is below 0.1%, it can hardly be detected by qPCR [10]. Many researchers suggest that sensitive detection of cfDNA mutations can be accomplished using droplet digital PCR (ddPCR) and next-generation sequencing (NGS) [11–13]; however, mutations with less than 0.1% allele frequency can be randomly detected using current techniques [14]. Therefore, strategies to improve the detection capability of clinically significant mutant alleles with exceptionally low copy numbers among circulating nucleic acids is needed [12].

Recently, clustered regularly interspaced short palindromic repeats (CRISPR)/CRISPR-associated protein 9 (Cas9) system has been introduced in the molecular diagnostic field to improve detection capability. Some applications have used the CRISPR system to specifically cleave non-target DNAs to increase the proportion of target DNA, which leads to increased analytical sensitivity [15–18]. Other techniques using the CRISPR system suggest mutant enrichment by specifically sorting out the target region by either target cleavage or by using a deactivated Cas9 (dCas9) with immunomagnetic separation. The enriched ctDNA obtained using the CRISPR/Cas9 system demonstrated an increased number of mutant allele copies compared to those from conventionally extracted ctDNA [19–21]. Active CRISPR/Cas9 is a versatile and precise tool for gene editing and targeting [22]. The final 20 base pairs of the single guide RNA (sgRNA) can be designed to target sites that contain the protospacer-adjacent motif (PAM) without any significant cross-reactivity or off-target effects [23, 24].

Building on advances in the CRISPR system, we introduced a new mutant enrichment technique called CRISPR system combined with post-PCR cfDNA (CRISPR-CPPC) to test cfDNA samples of patients with NSCLC having extremely low mutant allele copies to detect the T790M mutation.

Methods

Study design

We developed a new mutant enrichment technology, CRISPR-CPPC, and optimized it to increase its diagnostic sensitivity. We validated CRISPR-CPPC with reference standards of mutant alleles and cfDNA

from patients with NSCLC who had clinically progressed during or after EGFR-TKI treatment. The analytical performance of detecting *EGFR* T790M (NM_005228.4:c.2369C > T, p.Thr790Met) was evaluated by comparing the results of ddPCR with CRISPR-CPPC to those without CRISPR-CPPC. The study flowchart is shown in Supplemental Fig. 1. The CRISPR-CPPC comprises the following three steps: (1) cfDNA PCR, (2) assembly of post-PCR cfDNA and CRISPR/Cas9 complex, and (3) enrichment of the target DNA template. After CRISPR-CPPC, the target DNA can be detected using a variety of downstream applications. In this study, we used ddPCR as a downstream application for detecting T790M. A schematic representation of CRISPR-CPPC and sgRNA target positions is shown in Fig. 1 and Supplemental Fig. 2.

Patients

A total of 60 samples were collected from 51 patients who required *EGFR* gene mutation testing using Roche cobas® EGFR Mutation Test v2. The patients were admitted to two hospitals: Gangnam Severance Hospital and Severance Hospital located in Seoul, South Korea, from June 2018 to October 2020. Only patients with *EGFR*-mutated NSCLC who had clinically progressed during or after at least one first- or second-generation EGFR-TKI treatment cycle were included. Eight patients underwent one or two follow-up *EGFR* mutation tests. For all patients, *EGFR* genotyping was performed on the initial tissue biopsy obtained at the time of diagnosis. The study was approved by the Institutional Review Board of Gangnam Severance Hospital (IRB no. 3-2019-0393) and Severance Hospital (IRB no. 1-2019-0092). All patients provided written informed consent for specimen collection and genetic analysis. The need for the informed consent of the participants for reviewing medical records was waived on the condition that the research involves no more than minimal risk to the patients and their privacy.

Preparation Of Cfdna

Blood samples were collected in vacutainer tubes containing EDTA or cfDNA collection tubes with a cell stabilizer, Cell-Free DNA BCT (Streck, La Vista, NE, USA). Blood samples were centrifuged at 1,600 ×g for 10 min at 4°C, followed by a second high-spin centrifugation at 16,000 ×g for 10 min to separate the plasma from the peripheral blood cells. The plasma supernatant was stored at − 80°C until cfDNA extraction. The MagMAX Cell-Free DNA Isolation Kit (Thermo Fisher Scientific, Waltham, MA, USA) was used to extract cfDNA. The concentration and size distribution of the nucleic acids were assessed using a 2200 TapeStation Instrument (Agilent Technologies, Santa Clara, CA, USA) with an Agilent High Sensitivity D1000 ScreenTape System (Agilent Technologies, Santa Clara, CA, USA).

CRISPR-CPPC

cfDNA PCR

We designed the T790M primer sets for cfDNA PCR. Primer sequences are presented in Table 1. Cell-free DNA samples were processed by PCR before reacting with CRISPR/Cas9. PCR conditions were as follows: 95°C for 5 min, followed by 35 cycles of 95°C for 30 s, 62°C for 30 s, and 72°C for 1 min.

Table 1
EGFR T790M primer information

sgRNA*	forward	5'-TAATACGACTCACTATAGATCATGCAGCTCATGCCC-3'
	reverse	5'-TTCTAGCTCTAAAACAAGGGCATGAGCTGCATGAT-3'
cfDNA PCR†	forward	5'-CATGCGAAGCCACACTGAC-3'
	reverse	5'-CGGACATAGTCCAGGAGGCA-3'
*EGFR T790M primer for sgRNA.		
†Primer for cfDNA PCR. The expected product size was 164 bp.		
Abbreviations: sgRNA, single guide RNA; cfDNA, cell-free DNA		

Biotinylated sgRNA construction

The primer information for sgRNA is shown in Table 1. The sgRNA template was synthesized and purified using the GeneArt™ Precision gRNA Synthesis Kit (Thermo Fisher Scientific, Waltham, MA, USA) according to the manufacturer's instructions, but we elongated the incubation time to 4 h for *in vitro* gRNA transcription. The yield of sgRNA was measured using the Qubit RNA BR Assay kit (Thermo Fisher Scientific, Waltham, MA, USA) to confirm that its yield was within the 10 to 40 μg range. The 3'-end of sgRNA was biotinylated using the Pierce™ RNA 3'-End Biotinylation Kit (Thermo Fisher Scientific, Waltham, MA, USA). The reactions were incubated overnight at 16°C to increase efficiency.

CRISPR/Cas9 complex with post-PCR cfDNA

A CRISPR/Cas9 complex was constructed using biotinylated sgRNA, Cas9 nuclease, *Streptococcus pyogenes* (New England Biolabs, Ipswich, MA, USA), and the PCR product of the cfDNA samples. The most optimal enrichment condition for CRISPR-CPPC appeared to be a 5:1 molar ratio of biotinylated sgRNA to Cas9 protein in 20 μL of Cas9 reaction, which led to a molar ratio of 1:400 of post-PCR cfDNA to Cas9 complex. The CRISPR/Cas9 complex and post-PCR cfDNA were incubated at 37°C for 2 h in a thermocycler. Cas9 complexes trapping the target DNA were bound to the Dynabeads® MyOne™ Streptavidin C1 superparamagnetic beads (Thermo Fisher Scientific, Waltham, MA, USA) and released by heating to 65°C.

The methods of ddPCR, qPCR, NGS were written in Supplemental method.

Validation Of Crispr-cppc (Dup: Abstract ?)

Before using CRISPR-CPPC for patient cfDNA samples, the method was validated using Multiplex I cfDNA Reference Standards (Horizon Discovery, Cambridge, United Kingdom), which included wild-type cfDNA with mutant allele frequencies of 5%, 1%, and 0.1%. Healthy control and DNA-free samples were also analyzed. After performing the entire CRISPR-CPPC process, ddPCR was performed.

Data analysis

Quantification of the number of T790M mutant copies in the reaction was achieved by counting the number of positive and negative droplets. The limit of detection (LOD) was determined as the lowest copy number concentration above the 95% confidence interval (CI) of the wild-type control. The 95% CI was determined using the Poisson model and CLSI EP 17-A2 [25–28]. Based on the assessment of the limit of blank (LOB) and LOD, CRISPR-CPPC assays were considered positive if the measured events were ≥ 6 events/assay and negative if the events within a gated region were < 6 events/assay (Supplemental Table 1).

Statistical analysis

Statistical analysis was performed using Microsoft Excel 2016 (Microsoft Corporation, Redmond, WA, USA). Overall percent agreement (OPA), negative percent agreement (NPA), and positive percent agreement (PPA) were calculated as described in the CLSI guidelines [29]. Data are presented using 95% CIs and two-sided *P*-values. Statistical significance was set at $P \leq 0.05$.

Results

Patient characteristics

The characteristics of patients with *EGFR*-mutated NSCLC who had clinically progressed after EGFR-TKI treatment are described in Table 2. The median age was 62 years (range, 39–83 years), and thirty-six patients (70.6%) were females. Forty-three out of fifty-one patients had stage IV disease (84.3%). Thirty patients (58.8%) had exon 19 deletion, eighteen patients (35.3%) had L858R point mutation, two patients (3.9%) had S768I point mutation, one patient (2.0%) had L861Q point mutation, and one patient (2.0%) had G719S point mutation. Ten patients (19.6%) received erlotinib therapy, thirteen (25.5%) received afatinib, and twenty-seven (52.9%) received gefitinib therapy. One patient (2.0%) received gefitinib and erlotinib therapy at different time points. The median months of time period from the start of TKI to the sample collection for EGFR testing was 17.5 months (range, 2–72 months).

Table 2
Patient characteristics

Characteristics	No. of Patients
	n = 51 (100%)
Age, median (range), years	62 (39–83)
Sex	
Female	36 (70.6%)
Male	15 (29.4%)
Histologic type	
Adenocarcinoma	50 (98.0%)
Squamous cell carcinoma	1 (2.0%)
Tumor stage	
IB	2 (3.9%)
IIIA	3 (5.9%)
IIIB	3 (5.9%)
IVA	21 (41.2%)
IVB	22 (43.1%)
M category*	
M1a	13 (25.5%)
M1b	10 (19.6%)
M1c	27 (52.9%)
M1a + M1c†	1 (2.0%)
Tissue EGFR genotyping	

* The information of M category was reclassified at the time of EGFR testing. M category was based on the 8th TMN edition. M1a: lung metastases or pleural/pericardial malignant effusion or nodules; M1b: a single metastatic lesion in a single distant organ; M1c: multiple lesions in a single organ or multiple lesions in multiple organs

†The M category of patient G (Supplemental Table 7) was M1a at first EGFR testing. M stage was reclassified to M1c at second EGFR testing.

‡1 patient had both exon 19 deletion and L858R

Abbreviation: TKI, tyrosine kinase inhibitor

Characteristics	No. of Patients
	n = 51 (100%)
Exon 19 deletion	29 (56.9%)
L858R	17 (33.3%)
S768I	2 (3.9%)
L861Q	1 (2.0%)
G719S	1 (2.0%)
Exon 19 deletion + L858R‡	1 (2.0%)
Previous EGFR-TKI therapy	
Erlotinib	10 (19.6%)
Afatinib	13 (25.5%)
Gefitinib	27 (52.9%)
>1 EGFR-TKIs	1 (2.0%)
* The information of M category was reclassified at the time of EGFR testing. M category was based on the 8th TMN edition. M1a: lung metastases or pleural/pericardial malignant effusion or nodules; M1b: a single metastatic lesion in a single distant organ; M1c: multiple lesions in a single organ or multiple lesions in multiple organs	
†The M category of patient G (Supplemental Table 7) was M1a at first EGFR testing. M stage was reclassified to M1c at second EGFR testing.	
‡1 patient had both exon 19 deletion and L858R	
Abbreviation: TKI, tyrosine kinase inhibitor	

Validation Of Crispr-cppc

The analytical sensitivity of CRISPR-CPPC was evaluated using the Multiplex I cfDNA Reference Standard with allele frequencies of 5%, 1%, and 0.1% (Horizon Discovery, Cambridge, United Kingdom). The expected copy number of mutant alleles (3–109 copies) and the actual copy number of mutant alleles observed in these samples are presented in Table 3. The positive detection of mutant DNA after CRISPR-CPPC was approximately 2–6 times higher than the expected copies of mutant DNA. After mutant enrichment, the allele frequency was approximately 1.6–3.7 times higher than the expected allele frequency.

Table 3
Analytical sensitivity of CRISPR-CPPC in detecting *EGFR* T790M mutation

Reference Materials (T790M)	Expected allele frequency (%)*	Expected copies of mutant DNA per sample*	Expected copies of wild-type DNA per sample*	ddPCR after CRISPR-CPPC Detection positive (≥ 6 events/assay)		
				Observed Mutant allele frequency (%)	Copies of mutant DNA per sample	Copies of wild-type DNA per sample
5% Multiplex I cfDNA Reference Standard (HD777), 20 ng/µL	4.9	109	2120	8.8	231	2409
1% Multiplex I cfDNA Reference Standard (HD778), 20 ng/µL	1.1	24	2256	1.7	60	3376
0.1% Multiplex I cfDNA Reference Standard (HD779), 20 ng/µL	0.1	3	2228	0.5	19	3842

* Expected allele frequency and copy number of wild-type and mutant DNA measured using ddPCR were provided by the manufacturer.

Abbreviations: cfDNA, cell-free DNA; CRISPR-CPPC, CRISPR system combined with post-PCR cfDNA; ddPCR, droplet digital PCR

A comparison of qPCR, ddPCR, and ddPCR with CRISPR-CPPC assay

Sixty samples from fifty-one patients were analyzed. All samples were subjected to qPCR, ddPCR and CRISPR-CPPC assay for detecting T790M (Supplemental Table 2). Samples that tested positive for T790M through two or more of the experimental methods (qPCR from cfDNA or tissue, NGS, ddPCR, and CRISPR-CPPC) were considered to be true positives (Supplemental Table 3). According to Kim et al., ddPCR without CRISPR-CPPC was considered positive if the measured events were ≥ 2 events/assay and negative if the events within a gated region were < 2 events/assay [30]. Based on the results of multiple assays, the sensitivities of CRISPR-CPPC and ddPCR were 92.0% and 64.0%, respectively (Supplemental Table 3). The PPA (%), NPA (%), and OPA (%) of CRISPR-CPPC and ddPCR compared to the qPCR results are presented in Supplemental Table 4. Compared to qPCR, CRISPR-CPPC and ddPCR showed 100% and 75% PPA, respectively. CRISPR-CPPC detected T790M variants from 15 samples whose T790M mutations were not detected by qPCR. (Supplemental Table 4). When compared to ddPCR, the PPA (%),

NPA (%), and OPA (%) was 88.2%, 62.8 and 70.0%, respectively. (Supplemental Table 5). Eighteen samples showed discordant results between CRISPR-CPPC and ddPCR (Supplemental Table 6). CRISPR-CPPC detected T790M mutant alleles in sixteen T790M-negative samples by ddPCR, and ddPCR detected T790M in two T790M-negative samples by CRISPR-CPPC (sample No. 12 & 47). (Supplemental Table 5 & Supplemental Table 6). These two samples underwent further testing by NGS, which showed that one sample was T790M-positive with an allele frequency of 0.2% and the other was T790M-negative. The final clinical diagnosis of clinical progression was made by oncologists based on integration of patients' medical history and radiological findings. The researchers retrospectively reviewed the participant's medical records, including the final clinical diagnosis. Table 4 presents the analytical performance of CRIPSR-CPPC and ddPCR based on the results of multiple assays and final clinical diagnoses. The sensitivity and specificity of CRISPR-CPPC were increased up to 93.9% and 100.0%, respectively.

Table 4
Analytical performance of assays for detecting T790M mutation depending on clinical diagnosis

Method	T790M mutation was confirmed with multiple studies and or/and clinical diagnosis*			Sensitivity (95% CI)	Specificity (95% CI)	Accuracy (95% CI)
	Results	Pos (n = 33)	Neg (n = 27)			
ddPCR	Pos	16	1	48.5% (30.8–66.5%)	96.3% (81.0–99.9%)	70.0% (56.8–81.2%)
	Neg	17	26			
CRISPR-CPPC	Pos	31	0	93.9% (79.8–99.3%)	100.0% (87.2–100.0%)	96.7% (88.5–99.6%)
	Neg	2	27			

*T790M detected by more than one method (qPCR from cfDNA or tissue, NGS, ddPCR, CRISPR-CPPC) simultaneously is considered “true positive.” “Clinical diagnosis-T790M-positive” was defined when clinical history and image interpretation supported that a positive T790M result would be close to a true positive. Image interpretation was performed only for CRISPR-CPPC-positive samples.

Abbreviations: Pos, positive; Neg, negative; CI, confidence interval; CRISPR-CPPC, CRISPR system combined with post-PCR cfDNA; ddPCR, droplet digital PCR; qPCR, real-time PCR; NGS, next-generation sequencing

Ultra-sensitive Detection Of Crispr-cppc

A comparison of the allele frequency and positive calls of sixty samples is shown in Supplemental Table 2. Most samples showed approximately 1.2–13-times higher allele frequencies with the use of CRISPR-CPPC. In addition, approximately 1.6–562-times more positive calls were detected with the use of CRISPR-CPPC. The copy number comparison between pairs was statistically significant, with a *P*-value of < 0.0001, using the Wilcoxon signed-rank test.

We evaluated the performance of CRISPR-CPPC using the samples containing low copies of T790M mutant alleles from patients with *EGFR*-mutated NSCLC who had clinically progressed after EGFR-TKI

treatment. The distribution of T790M copies according to detecting assays was depicted in Supplemental Fig. 3. The overall T790M positive copy number differences between CRISPR-CPPC and ddPCR are shown in Fig. 2. Figure 2 shows the trend of CRISPR-CPPC increasing the T790M positive copy numbers compared to ddPCR without CRISPR-CPPC, except for sample number 47. Among 51 samples with ≤ 10 copies of T790M alleles based on ddPCR, the positive T790M rate of ddPCR and CRISPR-CPPC was 15.7% (n = 8 / 51) and 45.1% (n = 23 / 51), respectively (Supplemental Fig. 3 & Supplemental Table 2). CRISPR-CPPC showed improved sensitivity of detecting T790M, notably in samples with T790M-low copies or T790M-negative by ddPCR.

The monitoring EGFR T790M in patient samples using CRISPR-CPPC

Among the 51 patients, eight patients had one or two follow-up *EGFR* mutation tests using the Roche cobas® EGFR Mutation Test v2. As shown in Supplemental Table 7, patients E, G, and H had a follow-up test to detect T790M using CRISPR-CPPC, but qPCR was unable to detect T790M. Using ddPCR, 0, 3, and 0 positive calls with a respective allele frequency (%) of 0, 0.3, and 0 were detected. Using CRISPR-CPPC in the first sample from patient H, the T790M variant was detected with six positive calls with an allele frequency (%) of 0.1. In the second sample from patient E and patient G, T790M was detected with eight and nine positive calls and an allele frequency (%) of 0.2 and 0.3, respectively. These results indicate that only CRISPR-CPPC could detect exceptionally low copies of T790M in patient samples.

Discussion

In the routine process of treating patients with NSCLC, a great deal of effort is devoted to detecting *EGFR* mutations. Of late, clinical trials for many third-generation TKIs are underway [31, 32]. As the application of the mutation detection of cfDNA increases and becomes important in the field of precision medicine, the need for more sensitive mutation detection remains. A mutant enrichment technique combined with a sensitive detection tool is a feasible solution. In this study, we described a CRISPR-CPPC method for T790M mutant enrichment in cfDNA and demonstrated significant improvements in mutation detection capability in both commercial cfDNA reference standards and patient samples. There have been several approaches to mutation enrichment using CRISPR/Cas9 [19, 20], but most of them have not been tested in multiple authentic patient samples using ddPCR as a downstream application.

We evaluated the clinical applicability of CRISPR-CPPC by establishing a clinical cutoff. CRISPR-CPPC technology does not miss the T790M variants detected by qPCR. In addition, it allows the detection of T790M in patients with low copy numbers, even in samples in which T790M had not previously been detected by qPCR. Using CRISPR-CPPC, T790M was detected in total of 31 (51.7%) including additional 15 samples (Supplemental Table 4). Furthermore, CRISPR-CPPC detected the T790M mutation in 16 samples that had been previously identified as T790M mutation-negative by ddPCR (Supplemental Table 5). Two samples showed discordant results from ddPCR and CRISPR-CPPC; both samples were positive by ddPCR but negative by CRISPR-CPPC. NGS results indicated that one sample was T790M-negative and the other sample was T790M-positive, with an allele frequency of 0.2% (Supplemental

Table 5). CRISPR-CPPC may not have detected T790M in the second sample because < 0.1 ng of cfDNA sample was used during the PCR step, despite the sample having a low concentration of extracted cfDNA. The T790M mutant copy may have not been amplified because of the lower amount of DNA input for the PCR step (Supplemental Table 6). If a sufficient amount of cfDNA was used, CRISPR-CPPC may have been able to detect T790M in the second sample.

NGS tests were conducted on either some patient samples requested by clinicians or some discordant cases to determine whether they were true positives (Supplemental Table 6). One case (sample number 32) was shown to be T790M-negative by both ddPCR and CRISPR-CPPC (Supplemental Table 2), but NGS and tissue genotyping showed that the case was T790M-positive with an allele frequency of 0.2%. Both ddPCR and CRISPR-CPPC failed to detect T790M in this case, likely because cfDNA samples extracted from the stored plasma. In this study, stored plasma was used, and hence, was not as fresh as when NGS was conducted. cfDNA extracted from fresh plasma may improve the sensitivity of CRISPR-CPPC. The evaluation of cases with discordant results between ddPCR and CRISPR-CPPC indicates that CRISPR-CPPC can detect T790M with 93.9% sensitivity and 100% specificity in patients with a progressive disease along with the additional evidence of imaging interpretation. The sensitivity of CRISPR-CPPC increased 45.4% than that of ddPCR (Table 4). However, the true positives of these discordant cases were determined by oncologists based on patients' clinical histories and image interpretations. Therefore, further investigation by matching the results of NGS and CRISPR-CPPC from more samples should be conducted to confirm the diagnostic utility of CRISPR-CPPC.

CRISPR-CPPC technology requires further refinement prior to routine use; however, the CRISPR-CPPC has demonstrated several advantages: First, it is easy to use as long as the target primer is designed. Second, it can successfully enrich samples with a low number of mutant copies (< 10 copies/mL). Third, it can clarify the results in samples that previously had borderline results. Fourth, based on the experiment, enrichment reactions can be performed with the same amount (approximately 0.4 ng) of post-PCR cfDNA, indicating that CRISPR-CPPC can become a standardized process.

This study has several limitations. CRISPR-CPPC was hybridized with ddPCR because of its superior or non-inferior capability of sensitive variant detection compared to qPCR or NGS. Although this study demonstrated the better capability of sensitive detection compared to ddPCR without CRISPR-CPPC, further studies on the hybridization of CRISPR-CPPC to other downstream applications are required for future use. Furthermore, the pre-amplification step by PCR is added before reacting with CRISPR/Cas9; however, as shown in supplement table 8, mutant enrichment with CRISPR/Cas9 is an essential step for improving sensitivity even after the pre-amplification process. In addition, along with the amplification of the mutant copies, wild copies were also amplified, which led to the inclusion of the dilution step for reacting post-PCR cfDNA with the Cas9 complex. We tried to eliminate the dilution step by changing the PCR conditions (such as decreasing the number of cycles); however, the optimal conditions for mutant detection were not met without retaining the PCR and dilution steps. CRISPR-CPPC requires a PAM sequence to assemble the CRISPR/Cas9 complex; however, the PAM sequence (5'-NGG-3') can be found on average 8–12 bp in the human genome [21, 23, 33]. Therefore, this would not greatly hamper the

application of CRISPR-CPPC to the human genome. Finally, CRISPR-CPPC cannot be used for patient monitoring because its quantitative application has not yet been evaluated. Therefore, the results of CRISPR-CPPC should only be considered qualitatively. Although this approach met the study's original purpose of enriching low mutant copies to render them detectable, it needs to be developed as a quantitative tool to be used for both diagnostic and monitoring patient care purposes. Incorporating dead Cas9 into CRISPR-CPPC may solve this problem, but further study is required.

There have been many approaches to integrate the CRISPR system with detection assays to improve diagnostic ability. Instead of using CRISPR/Cas9, Kellner et al. used Cas13 and developed a protocol for Specific High Sensitivity Enzymatic Reporter UnLOCKing (SHERLOCK) nucleic acid detection; however, this system lacks the ability of absolute digital quantification [34]. Despite the need for further refinement of CRISPR-CPPC, this technology demonstrated that CRISPR/Cas9 can be used as a mutant enrichment tool with the capability of absolute quantification due to its integration with ddPCR. This study shows that the performance of CRISPR-CPPC is exceptionally better than that of any other currently available methods and that it can be easily used in clinical settings. Therefore, CRISPR-CPPC can be clinically applied to facilitate gene expression profiling, diagnosis, and the selection of appropriate treatment regimens.

Conclusions

In conclusion, the proposed CRISPR-CPPC technology is a useful mutant enrichment tool for the sensitive detection of target mutations. CRISPR-CPPC can enrich mutations without cleaving the target or non-targets but rather uses CRISPR/Cas9 to recognize targets. We demonstrated the capability of CRISPR-CPPC to detect low copy number mutations in the cfDNA of patients with TKI resistance, possibly caused by the T790M mutation, which is undetectable in the patients by current FDA-approved methods. Thus, CRISPR-CPPC can greatly contribute to diagnosis and the selection of appropriate treatment regimens by facilitating the sensitive detection of mutations in cfDNA.

Abbreviations

Cas9: CRISPR associated protein 9; cfDNA: cell-free DNA; CI: confidence interval; ctDNA: circulating tumor DNA; CRISPR-CPPC: CRISPR system combined post-PCR cfDNA; dCas9: deactivated Cas9; ddPCR: droplet digital PCR; EGFR: epidermal growth factor receptor; LOB: limit of blank; LOD: limit of detection; NGS: next-generation sequencing; NPA: negative percent agreement; NSCLC: non-small cell lung cancer; OPA: Overall percent agreement; PAM: protospacer-adjacent motif; PCR: polymerase chain reaction; PD: progressive disease; PPA: positive percent agreement; qPCR: real-time PCR; sgRNA: single guide RNA; TKI: tyrosine kinase inhibitor; WT: wild-type

Declarations

Ethics approval and consent to participate

The study was approved by the Institutional Review Board of Gangnam Severance Hospital (IRB no. 3-2019-0393) and Severance Hospital (IRB no. 1-2019-0092). All patients provided written informed consent for specimen collection and genetic analysis. The need for the informed consent of the participants for reviewing medical records was waived on the condition that the research involves no more than minimal risk to the patients and their privacy.

Consent for publication

All authors involved in the study had given their consent for submitting this article for publication.

Availability of data and materials

The data that support the findings of this study, contain clinical outcomes for which IRB requires approval prior to analysis. Therefore, the data are not publicly available. The data will be made available to authorized researchers who have obtained institutional review board (IRB) approv-al from their own institution and from Gangnam Severance Hospital, Yonsei University, Seoul, Republic of Korea IRB. For data access requests, please contact the corresponding author, Dr. Kyung-A Lee, email address: kal1119@yuhs.ac

Competing interests

The authors declare no conflicts of interest.

Funding

This study was supported by a faculty research grant of Yonsei University College of Medicine (6-2020-0129).

Author’s contributions

BK, YK and KAL conceived and designed the study. BK, YK, and JYC analyzed and interpreted the patient data. BK and YK equally contributed in writing the manuscript. SS, STL and KAL provided experiment resources and supervised this work. All authors read and approved the final manuscript.

Acknowledgements

The authors thank Medical Illustration & Design, part of the Medical Research Support Services of Yonsei University College of Medicine, for providing excellent support with medical illustrations.

References

1. Calabuig-Farinas S, Jantus-Lewintre E, Herreros-Pomares A, Camps C. Circulating tumor cells versus circulating tumor DNA in lung cancer-which one will win? Transl Lung Cancer Res. 2016;5(5):466–82.

2. Yi X, Ma J, Guan Y, Chen R, Yang L, Xia X. The feasibility of using mutation detection in ctDNA to assess tumor dynamics. Int J Cancer. 2017;140(12):2642–7.
3. Kustanovich A, Schwartz R, Peretz T, Grinshpun A. Life and death of circulating cell-free DNA. Cancer Biol Ther. 2019;20(8):1057–67.
4. Planchard D, Popat S, Kerr K, Novello S, Smit EF, Faivre-Finn C, et al. Metastatic non-small cell lung cancer: ESMO Clinical Practice Guidelines for diagnosis, treatment and follow-up. Ann Oncol. 2018;29(Suppl 4):iv192–237.
5. Soria JC, Ohe Y, Vansteenkiste J, Reungwetwattana T, Chewaskulyong B, Lee KH, et al. Osimertinib in Untreated EGFR-Mutated Advanced Non-Small-Cell Lung Cancer. N Engl J Med. 2018;378(2):113–25.
6. Mok TS, Wu YL, Ahn MJ, Garassino MC, Kim HR, Ramalingam SS, et al. Osimertinib or Platinum-Pemetrexed in EGFR T790M-Positive Lung Cancer. N Engl J Med. 2017;376(7):629–40.
7. Buder A, Setinek U, Hochmair MJ, Schwab S, Kirchbacher K, Keck A, et al. EGFR Mutations in Cell-free Plasma DNA from Patients with Advanced Lung Adenocarcinoma: Improved Detection by Droplet Digital PCR. Target Oncol. 2019;14(2):197–203.
8. Buder A, Hochmair MJ, Schwab S, Bundalo T, Schenk P, Errhalt P, et al. Cell-Free Plasma DNA-Guided Treatment With Osimertinib in Patients With Advanced EGFR-Mutated NSCLC. J Thorac Oncol. 2018;13(6):821–30.
9. Li X, Zhou C. Comparison of cross-platform technologies for EGFR T790M testing in patients with non-small cell lung cancer. Oncotarget. 2017;8(59):100801–18.
10. Watanabe M, Kawaguchi T, Isa S, Ando M, Tamiya A, Kubo A, et al. Ultra-Sensitive Detection of the Pretreatment EGFR T790M Mutation in Non-Small Cell Lung Cancer Patients with an EGFR-Activating Mutation Using Droplet Digital PCR. Clin Cancer Res. 2015;21(15):3552–60.
11. Sorber L, Zwaenepoel K, Deschoolmeester V, Van Schil PE, Van Meerbeeck J, Lardon F, et al. Circulating cell-free nucleic acids and platelets as a liquid biopsy in the provision of personalized therapy for lung cancer patients. Lung Cancer. 2017;107:100–7.
12. Elazezy M, Joosse SA. Techniques of using circulating tumor DNA as a liquid biopsy component in cancer management. Comput Struct Biotechnol J. 2018;16:370–8.
13. Liang Z, Cheng Y, Chen Y, Hu Y, Liu WP, Lu Y, et al. EGFR T790M ctDNA testing platforms and their role as companion diagnostics: Correlation with clinical outcomes to EGFR-TKIs. Cancer Lett. 2017;403:186–94.
14. Volckmar AL, Sültmann H, Riediger A, Fioretos T, Schirmacher P, Endris V, et al. A field guide for cancer diagnostics using cell-free DNA: From principles to practice and clinical applications. Genes Chromosomes Cancer. 2018;57(3):123–39.
15. Montefiori L, Hernandez L, Zhang Z, Gilad Y, Ober C, Crawford G, et al. Reducing mitochondrial reads in ATAC-seq using CRISPR/Cas9. Sci Rep. 2017;7(1):2451.
16. Gu W, Crawford ED, O'Donovan BD, Wilson MR, Chow ED, Retallack H, et al. Depletion of Abundant Sequences by Hybridization (DASH): using Cas9 to remove unwanted high-abundance species in sequencing libraries and molecular counting applications. Genome Biol. 2016;17:41.

17. Jia C, Huai C, Ding J, Hu L, Su B, Chen H, et al. New applications of CRISPR/Cas9 system on mutant DNA detection. Gene. 2018;641:55–62.
18. Lee SH, Yu J, Hwang GH, Kim S, Kim HS, Ye S, et al. CUT-PCR: CRISPR-mediated, ultrasensitive detection of target DNA using PCR. Oncogene. 2017;36(49):6823–9.
19. Lee J, Lim H, Jang H, Hwang B, Lee JH, Cho J, et al. CRISPR-Cap: multiplexed double-stranded DNA enrichment based on the CRISPR system. Nucleic Acids Res. 2019;47(1):e1.
20. Aalipour A, Dudley JC, Park SM, Murty S, Chabon JJ, Boyle EA, et al. Deactivated CRISPR Associated Protein 9 for Minor-Allele Enrichment in Cell-Free DNA. Clin Chem. 2018;64(2):307–16.
21. Song J, Kim S, Kim HY, Hur KH, Kim Y, Park HG. A novel method to detect mutation in DNA by utilizing exponential amplification reaction triggered by the CRISPR-Cas9 system. Nanoscale. 2021;13(15):7193–201.
22. Wassef M, Luscan A, Battistella A, Le Corre S, Li H, Wallace MR, et al. Versatile and precise gene-targeting strategies for functional studies in mammalian cell lines. Methods. 2017;121–122:45–54.
23. Cong L, Ran FA, Cox D, Lin S, Barretto R, Habib N, et al Multiplex genome engineering using CRISPR/Cas systems. Science. (1979). 2013;339(6121):819 – 23.
24. Shen B, Zhang W, Zhang J, Zhou J, Wang J, Chen L, et al. Efficient genome modification by CRISPR-Cas9 nickase with minimal off-target effects. Nat Methods. 2014;11(4):399–402.
25. Armbruster DA, Pry T. Limit of blank, limit of detection and limit of quantitation. Clin Biochem Rev. 2008;29(Suppl 1):49–52. Suppl 1(.
26. Milosevic D, Mills JR, Campion MB, Vidal-Folch N, Voss JS, Halling KC, et al. Applying Standard Clinical Chemistry Assay Validation to Droplet Digital PCR Quantitative Liquid Biopsy Testing. Clin Chem. 2018;64(12):1732–42.
27. Milbury CA, Zhong Q, Lin J, Williams M, Olson J, Link DR, et al. Determining lower limits of detection of digital PCR assays for cancer-related gene mutations. Biomol Detect Quantif. 2014;1(1):8–22.
28. CLSI. Evaluation of Detection Capability for Clinical Laboratory Measurement Procedures; Approved Guideline-Second Edition. CLSI document EP17-A2. Wayne: Clinical and Laboratory Standards Institute; 2012.
29. CLSI. User Protocol for Evaluation of Qualitative Test Performance; Approved Guideline-Second Edition. CLSI document EP12-A2. Wayne: Clinical and Laboratory Standards Institute; 2012.
30. Kim Y, Shin S, Kim B, Lee KA. Selecting short length nucleic acids localized in exosomes improves plasma EGFR mutation detection in NSCLC patients. Cancer Cell Int. 2019;19:251.
31. Nagasaka M, Zhu VW, Lim SM, Greco M, Wu F, Ou SI. Beyond Osimertinib: The Development of Third-Generation EGFR Tyrosine Kinase Inhibitors For Advanced EGFR + NSCLC. J Thorac Oncol. 2021;16(5):740–63.
32. Oxnard GR, Yang JC, Yu H, Kim SW, Saka H, Horn L, et al. TATTON: a multi-arm, phase Ib trial of osimertinib combined with selumetinib, savolitinib, or durvalumab in EGFR-mutant lung cancer. Ann Oncol. 2020;31(4):507–16.

33. Hsu PD, Scott DA, Weinstein JA, Ran FA, Konermann S, Agarwala V, et al. DNA targeting specificity of RNA-guided Cas9 nucleases. Nat Biotechnol. 2013;31(9):827–32.
34. Kellner MJ, Koob JG, Gootenberg JS, Abudayyeh OO, Zhang F. SHERLOCK: nucleic acid detection with CRISPR nucleases. Nat Protoc. 2019;14(10):2986–3012.

Figures

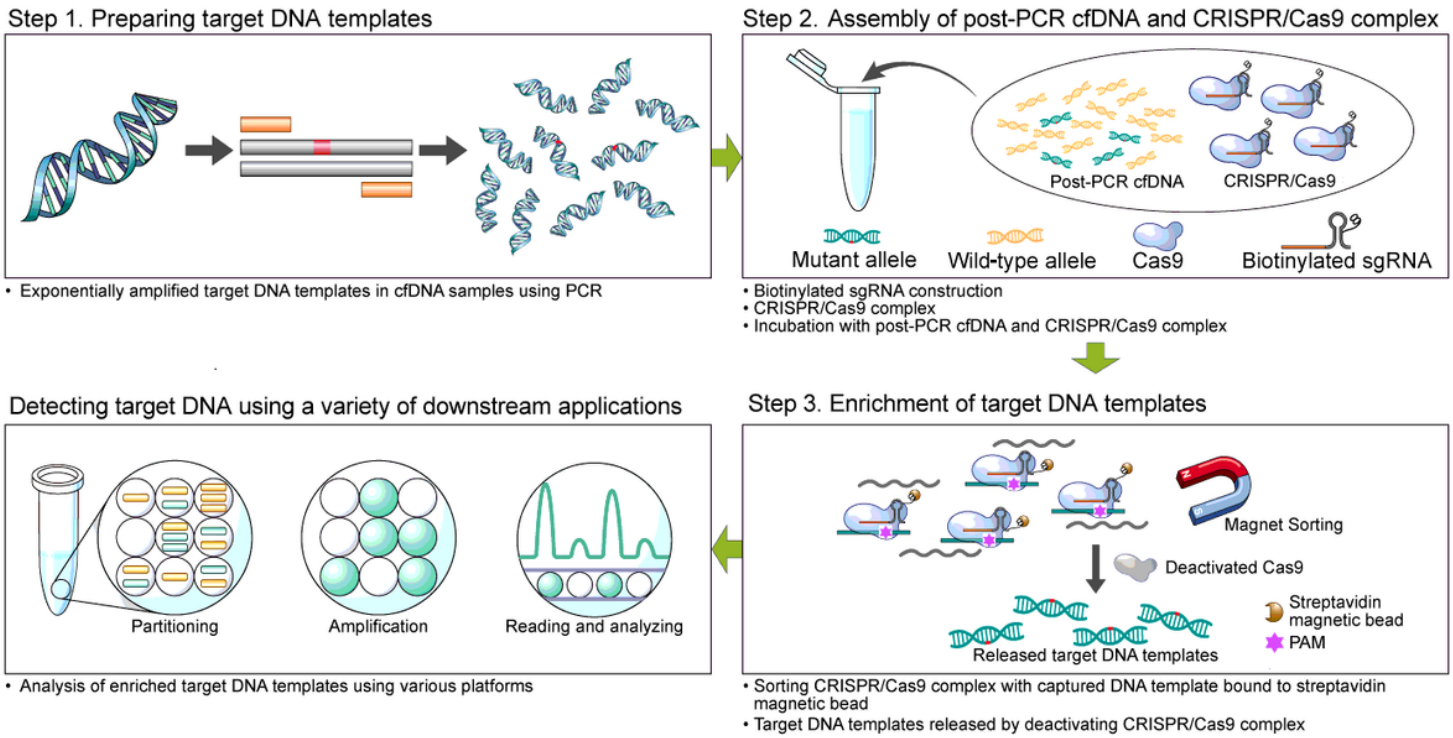

Figure 1

Schematic diagram of CRISPR-CPPC. CRISPR-CPPC comprises three steps: 1) cfDNA PCR, 2) assembly of post-PCR cfDNA and Cas9 complex, 3) enrichment of target DNA template. After CRISPR-CPPC, the target DNA can be detected using a variety of downstream applications, such as ddPCR.

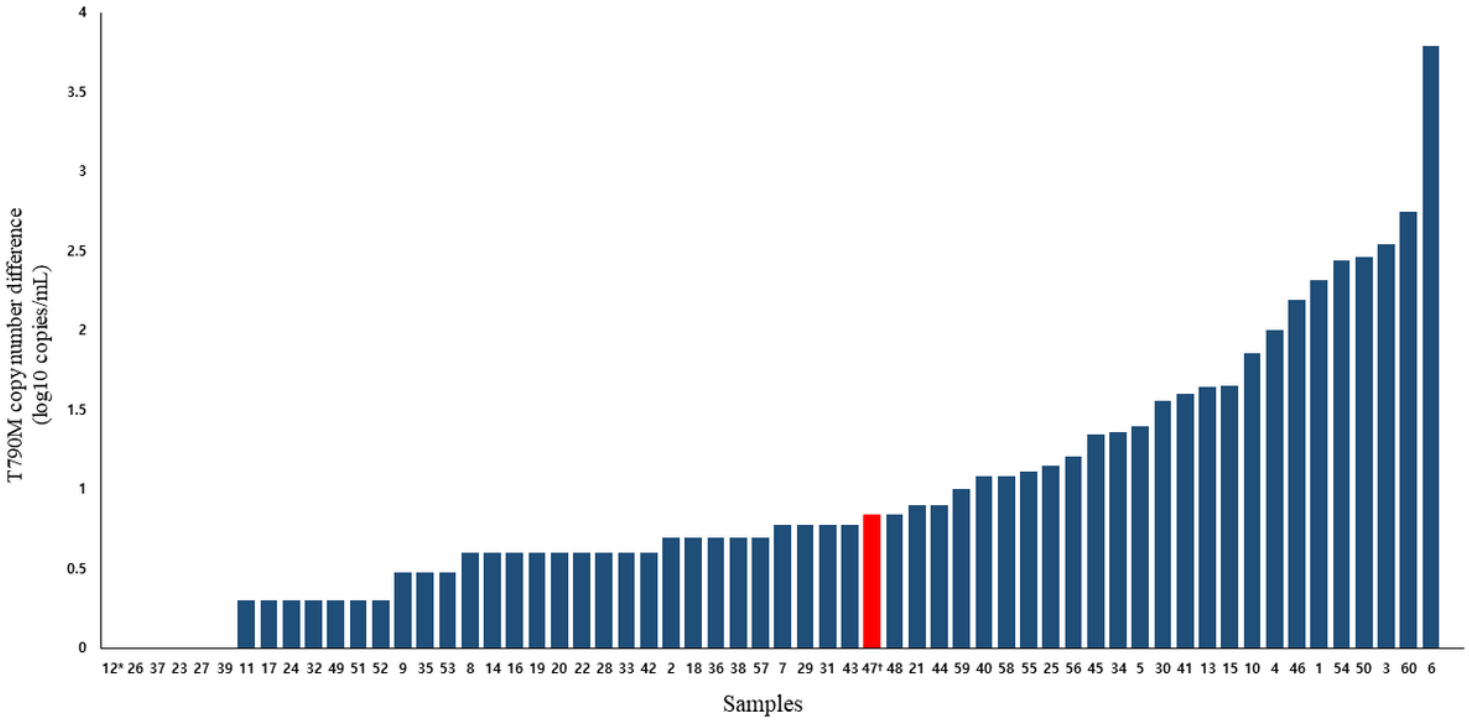

Figure 2

T790M-positive copy number differences between CRISPR-CPPC and ddPCR in all 60 samples: CRISPR-CPPC increased the T790M-positive copy numbers, except in sample number 47 (Supplemental Table 2). Seven samples with a copy difference of <1 were not expressed on the log10-scaled y-axis.

Supplementary Files

This is a list of supplementary files associated with this preprint. Click to download.

- supplemental.docx